



Kahramanmaraş Sütçü İmam University

Journal of Engineering Sciences



Geliş Tarihi : 15.03.2024
Kabul Tarihi : 02.04.2024

Received Date : 15.03.2024
Accepted Date : 02.04.2024

INVESTIGATION OF THE EFFECTIVENESS IN THE SOLID PHASE EXTRACTION STUDIES OF THE GRAPHENE HYBRIDS

GRAFEN HİBRİTLERİNİN KATI FAZ EKSTRAKSİYON ÇALIŞMALARINDAKİ ETKİNLİĞİNİN ARAŞTIRILMASI

Zaman MOHAMMED¹ (ORCID:0000-0002-3457-3953)
Derya Kılıçaslan² (ORCID: 0000-0001-7830-8214)
Muharrem KARABÖRK^{1*} (ORCID: 0000-0002-5996-6243)

¹Department of Chemistry, Kahramanmaraş Sütçü İmam University, Kahramanmaraş, 46050, Turkey

²Afsin Vocational School, Department of Chemistry and Chemical Processing Technologies, Kahramanmaraş Sütçü İmam University, Kahramanmaraş, Turkey

*Corresponding Author: M. Karabörk, mkarabork@ksu.edu.tr.

ABSTRACT

The objective of this study is to evaluate the effectiveness of using a graphene-based hybrid material as a substance that can attract and separate other substances in a solid-phase extraction process. The goal is to reduce the potential adverse effects of Pb(II) and Hg(II) metal ions on human health and the environment. Graphene oxide was produced on graphite using the Hummers process during the early phase, which involved the use of potent oxidizers. Afterwards, graphene oxide (GO) was treated with 3-(trimethoxycylene)propylamine to silanize it. Then, the silanized GO was combined with 3,5-dichloro-salisylaldehyde to create the graphen-Schiff base material. The structure of the compounds was determined at each stage of synthesis using a range of analytical techniques, such as UV-Vis spectroscopy, Fourier transform infrared spectroscopy, X-ray diffraction, scanning electron microscopy, transmission electron microscopy, thermogravimetric analysis, and energy dispersive X-ray spectroscopy. The study investigated the influence of pH, temperature, contact time, and other material characteristics on adsorption. The study demonstrated that the graphene-based hybrid material is highly efficient at adsorbing heavy metal ions from both waste and drinking water. This demonstrates the potential of graphene in environmental applications, as it can effectively remove heavy metal contaminants.

Keywords: Graphene oxide, graphene-based hybrid material, adsorption, heavy metals

ÖZET

Bu çalışmanın amacı, grafen bazlı hibrit bir malzemenin katı faz ekstraksiyon işleminde diğer maddeleri çekebilen ve ayırabilen bir madde olarak kullanılmasının etkinliğini değerlendirmektir. Amaç, Pb(II) ve Hg(II) metal iyonlarının insan sağlığı ve çevre üzerindeki potansiyel olumsuz etkilerini azaltmaktır. Grafen oksit, güçlü oksitleyicilerin kullanımını içeren ilk aşamada Hummers prosesi kullanılarak grafit üzerinde üretilmiştir. Daha sonra, GO silanize etmek için 3-(trimetoksisilen)propilamin ile muamele edilmiştir. Daha sonra silanize edilmiş GO, grafen-oksit-Schiff baz malzemesini oluşturmak için 3,5-dikloro-salisilaldehit ile birleştirildi. Bileşiklerin yapısı sentezin her aşamasında UV-Vis spektroskopisi, Fourier dönüşümlü kızılötesi spektroskopisi, X-ışını kırınımı, taramalı elektron mikroskopisi, transmisyon elektron mikroskopisi, termogravimetrik analiz ve enerji dağılımlı X-ışını spektroskopisi gibi bir dizi analitik teknik kullanılarak belirlendi. Çalışmada pH, sıcaklık, temas süresi ve diğer malzeme özelliklerinin adsorpsiyon üzerindeki etkisi araştırılmıştır. Çalışma, grafen bazlı hibrit malzemenin hem atık hem de içme suyundan ağır metal iyonlarını adsorbe etmede oldukça verimli olduğunu göstermiştir. Bu durum, ağır metal kirleticileri etkili bir şekilde uzaklaştırabildiği için grafenin çevresel uygulamalardaki potansiyelini göstermektedir.

Anahtar Kelimeler: Grafen oksit, ağır metaller, adsorpsiyon, grafen bazlı hibrit malzeme

ToCite: MOHAMMED, Z., & KILIÇASLAN, D., KARABÖRK, M., (2024). INVESTIGATION OF THE EFFECTIVENESS IN THE SOLID PHASE EXTRACTION STUDIES OF THE GRAPHENE HYBRIDS. *Kahramanmaraş Sütçü İmam Üniversitesi Mühendislik Bilimleri Dergisi*, 27(3), 1033-1043.

INTRODUCTION

Heavy metals are defined as naturally occurring elements with a higher density and a large atomic weight among metallic elements (Abd Elnabi et al., 2023). These metals are one of the most investigated pollutants that have been widely studied by researchers due to their toxicity (Ali et al., 2019; Masindi & Muedi, 2018). These naturally occurring elements in the environment, together with factors such as modern industrialization, urbanization, anthropogenic activities, and fertilizer use, have led to an increase in their environmental levels and therefore to high levels of exposure to living organisms (Ali et al., 2019; Balali-Mood et al., 2021).

Heavy metals include the most toxic metalloids, such as chromium, mercury, arsenic, cadmium, lead, nickel, copper, and zinc. However, the most common ones in the environment are chromium, manganese, nickel, lead, cadmium, copper, and zinc (Gabriel & Elena, 2022). Humans can come into contact with heavy metals as a result of industrial activities, and this contact can occur through various routes such as digestion, respiration, and dermal absorption (Ali et al., 2019). Heavy metals are categorized as essential or non-essential according to their function in biological systems. The presence of excessive amounts of these metals can cause physiological or morphological disorders and genetic mutations (Mitra et al., 2022).

The World Health Organization (WHO) classifies trace elements into three groups based on their importance and potential toxicity: essential elements (zinc, iodine, molybdenum, copper, selenium, and chromium), possibly essential elements (manganese, silicon, boron, vanadium, and nickel), and potentially toxic elements (lead, cadmium, fluorine, mercury, aluminum, arsenic, barium, lithium, and tin) (Bhattacharya et al., 2016; Aliasgharpour & Marjan, 2013).

Solid-phase extraction (SPE) and solid-phase microextraction (SPME) are sample preparation techniques used for the extraction of analytes from complex matrices. SPE is widely used in the extraction of heavy metals from environmental samples such as water, soil, and air because it offers an effective solution to the problems associated with phase separation and processing (Ingrassia et al., 2024; Zhou et al., 2023). On the other hand, SPME is a solvent-free extraction technique widely used for the determination of trace components in various samples, including beers (Lucena, 2023). SPME offers advantages such as cost-effectiveness, versatility, and automation, making it a popular choice for the analysis of aroma compounds, flavors, bad tastes, and exogenous contaminants in food and beverage samples (Pasupuleti & Huang, 2023). Both SPE and SPME techniques have been combined with atomic spectroscopy for the determination of heavy metals in environmental samples.

This study created a hybrid imine-graphene material to remove heavy metal ions like Pb(II) and Hg(II) from environmental water sources. Graphene oxide (GO) was first produced by oxidizing H₂SO₄ and KMnO₄ using the Hummers method. Silanizing GO using 3-(trimethoxysilyl)propylamine followed. The GO-Schiff basic material was made from silanized GO and 3,5-dichloro-salicylaldehyde. Compound structures were determined using various techniques, including UV-Vis, FT-IR, TGA, XRD, TEM, EDX, and SEM. Next, batch experiments were performed to study Pb(II) and Hg(II) ion adsorption in water. ICP-AES was used for the experiments.

MATERIAL AND METHOD

General Methods

The functional groups of compounds were determined after each treatment using X-ray powder diffraction, namely the Perkin-Elmer spectrum FT-IR/FT-FIR Spectrometer. Scanning Electron Microscopy and Energy Dispersive X-ray spectroscopy, namely using the SEM (Scanning Electron Microscope) ZEISS EVOLS10 and the EDX (Energy Dispersive X-ray Spectroscopy) Brulas123eV dedeluctor, was employed to determine the morphology and elemental composition of the nanocomposite. The phase identifications of the functionalized nanocomposite were conducted using a Philips X'Pert Pro X-ray diffractometer (XRD) for X-ray powder diffractions. The Perkin Elmar 2100 D/V model of Inductive Coupled Plasma Atomic Emission Spectroscopy (ICP-AES) was employed to analyze heavy metal ions in solutions treated with manufactured nano-substances. Thermogravimetric Analysis, also known as Thermal Gravimetric Analysis (TGA: EXSTARTG/DTA 6300), was employed to illustrate the characteristics of the synthesized nanomaterials. The SHIMADZU UV-1800, an Ultraviolet-Visible Spectroscopy instrument, was utilized to quantitatively determine the Graphene Oxide (GO) through emission and adsorption stages. The Transmission Electron Microscope (HRTEM: JEOL JEM-2100F) was employed to facilitate the imaging of the produced nanostructure and its attributes. The pH values of Pb(II) and Hg(II) metal ion solutions were determined using a pH meter (HANNA HI1221).

Graphene Oxide Synthesis

The synthesis of graphene oxide was achieved using the conventional Hummer's method as depicted in Figure 1 (Hummers et al., 1958). The procedure was separated into three distinct stages to enhance comprehension. The initial phase, referred to as cold treatment, involved dissolving 2 grams of graphite powder in 100 ml of H_2SO_4 and stirring the mixture in an ice bath for thirty min. Subsequently, 8 grams of potassium permanganate ($KMnO_4$) were gradually introduced into the solution to prevent any abrupt increase in temperature. Following the addition, the solution was allowed to incubate for a duration of 2 h in an ice bath. The color undergoes a transition from a dark gray shade to a green hue. Next, we proceeded to perform a heat treatment. The solution was agitated for a duration of 1 h at a temperature of $35^\circ C$ in a water bath. Subsequently, after the passage of 1 h, a gradual addition of 100 ml of distilled water took place. The solution's temperature increased and varied between 40 and $60^\circ C$. Furthermore, the color of the object changes from a dark color of green to a dark color of brown. Following the addition, the solution was once again placed in a warm water bath at a temperature of $35^\circ C$ and stirred using a magnetic stirrer for a duration of 1 h. Furthermore, the treatment was referred to as a hot application, wherein the solution was heated to a temperature of $95^\circ C$ using bath water. Once it reached that temperature, it was let to sit for 15 min. Subsequently, 300 ml of distilled water at ambient temperature and a 30% concentration of H_2O_2 were introduced. The solution's color transitioned from a reddish brown hue to a shade of yellowish brown. Ultimately, it came to a halt and remained still for a duration of 15 h. Upon observation the following morning, it was seen that the solution was undergoing gas release, and all the GOs were observed to be precipitating at the bottom of the beaker. The aqueous component of the solution was extracted, and GO was subjected to rinsing with a 5% HCl solution followed by pure water. Ultimately, it was necessary to allow it to desiccate at a location devoid of light (Hummers et al., 1958).

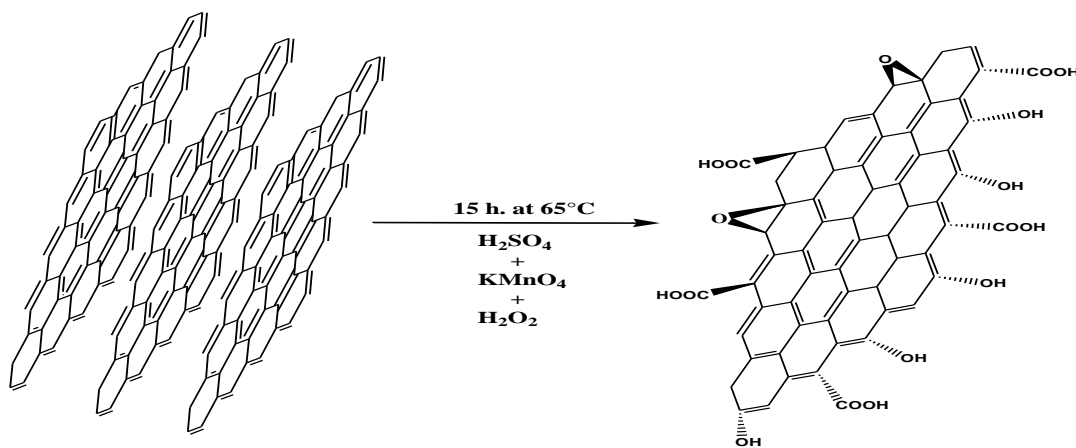


Figure 1. Graphene Oxide Synthesis Using Hummer's Method

Silanization of Graphene Oxide

2 grams of GO were measured, and then combined with 100 ml of anhydrous ethanol by reflux for a duration of one day (Jamali et al., 2006). After being stirred with dry ethanol under reflux for 24 h, 5 ml of 3-(triethoxysilyl-propyl)amine was added using ejection. The mixture was then stirred under reflux for a further 24 h at a temperature of $60-65^\circ C$. Ultimately, it was treated with 100 ml of ethanol to eliminate the remaining unreacted sylan molecules, rinsed with water, and dried. By adhering to this procedure, GO-3-(triethoxysilyl-propyl)amine shown in Figure 2 was acquired.

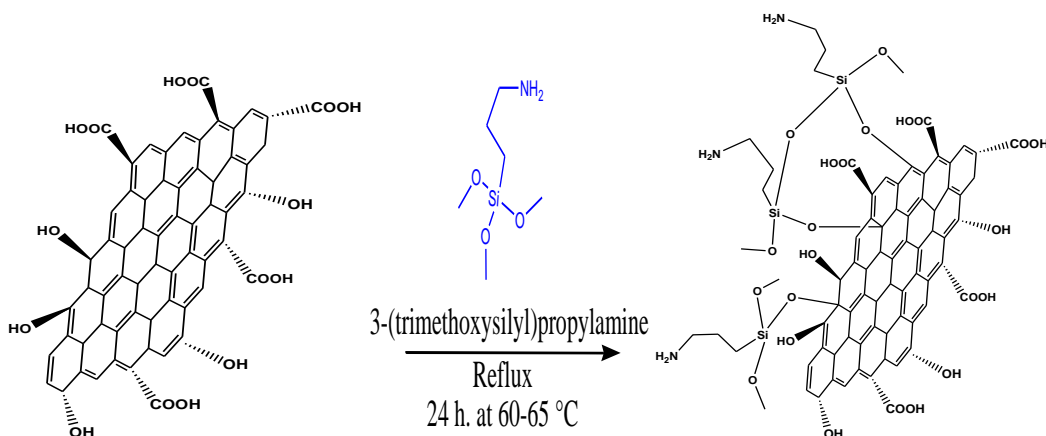


Figure 2. Graphene Oxide is Functionalized Using 3-(Triethoxysilyl-Propylamine)

Preparation of Graphene Oxide-Schiff Base Material

1 gram of GO-3-(triethoxysilyl-propylamine) was measured and combined with 1 gram of 3,5-dichloro-salicylaldehyde, which had been dispersed in 30 milliliters of ethanol in the flask. The mixture was then stirred for 30 h at a temperature of 60–65 °C under reflux conditions to produce GO-Si (3-propyl) 3,5-dichloro-salicylaldehyde, as depicted in Figure 3. Ultimately, the substance was allowed to reach the ambient temperature and cleansed with ethanol, subsequently subjected to a drying process at 40 °C in an oven (Hou et al., 2010).

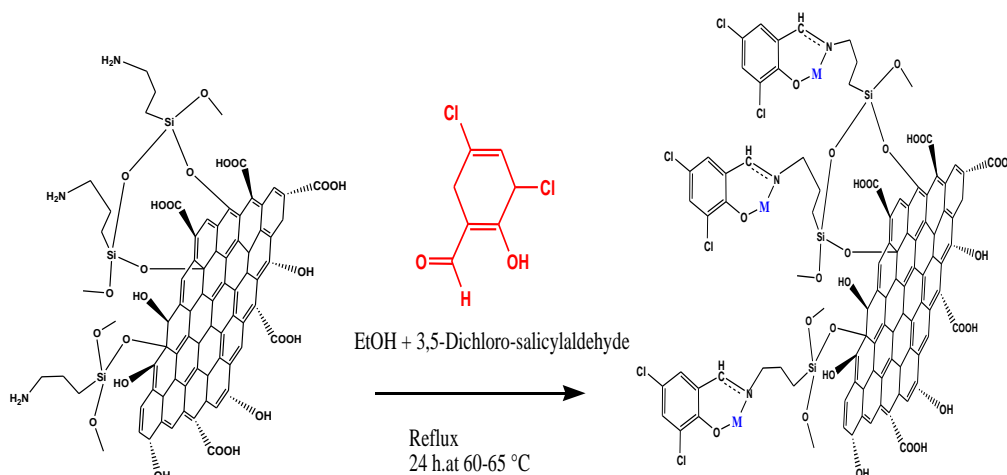


Figure 3. Preparation of GO-Schiff Base Material

RESULTS AND DISCUSSION

Characterization of Compounds

The UV-VIS spectrum of the standard GO is displayed in the Supplementary File (Fig. S1). Two weavers are visible at wavelengths of 235 and 325 nm. The electron transition of π - π^* aromatic rings is broad, whereas the other transition is lightly broad. These transitions indicate the presence of carbonyl groups, which are surrounded by the n- π^* electron transition on the graphene layer.

Graphene oxide: The functional groups, predominantly consisting of oxygen, were seen using FT-IR measurement, as depicted in Figure 4. Several peaks were seen at specific wavenumbers, namely 3433.44, 1723.34, 1631.66, 1414.48, 1226.89, 1058.25, and 837.34 cm^{-1} . These peaks indicate the presence of functional groups in GO. The prominent peak at 3433.44 cm^{-1} indicates the stretching movement of the O-H bond in CO-H groups and water molecules. The peak at 1723.34 cm^{-1} corresponds to the stretching of carboxyl groups (C=O). The peak at 1631.66 cm^{-1} is most likely due to the stretching of C=C bonds, while the bending of C-O-H bonds is observed at 1414.48 cm^{-1} . The peak at around 1226.89 cm^{-1} is likely associated with the stretching of the C-O bonds in the acyl and phenyl groups. The presence of alkoxy C-O-C bonds was detected at a wavenumber of 1058.25 cm^{-1} (Bal et al., 2024).

The silanized graphene oxide (Si-GO) was analyzed using FT-IR to identify the functional group patterns at specific wavenumbers: 3412.79, 2921.46, 2847.19, 1712.07, 1564.23, 1464.73, 1385.50, 1327.53, 1225.12, 1122.70, 1034.73, 919.80, 771.01, 691.78, and 614.49 cm^{-1} , as depicted in Figure 4. The presence of a broad OH peak and a CO-H stretch was seen at a wavenumber of 3412.79 cm^{-1} . The bands at 2921.46 and 2847.19 cm^{-1} correspond to the symmetric and asymmetric stretching of C-H bonds, respectively. The intense carbonyl C=O peak was observed at a wavenumber of 1712.07 cm^{-1} . The prominent peak at 1564.23 cm^{-1} is indicative of a carbon-carbon double bond (C=C). The signal observed at 1464.73 cm^{-1} is assigned to the CH₂ group, which does not contain any silicon (Si) atoms. The peaks observed at approximately 1385.50 cm^{-1} likely correspond to the bending motion of the hydroxyl (OH) group. The peak at 1327.53 cm^{-1} corresponds to the presence of C-O acyl groups in the band. The signal at 1225.12 cm^{-1} corresponds to the characteristic C-N bonds of amine groups. The vibrational frequencies of Si-O-C and Si-O-Si were measured as 1122.70 cm^{-1} and 1034.73 cm^{-1} , respectively. In addition, the Si-C band becomes visible at a frequency of 919.80 cm^{-1} . The Si-O-CH₃ peak was observed at a wavenumber of 771.01 cm^{-1} . Ultimately, the N-H summit experienced a modest elevation to 691.78 cm^{-1} .

The structure of the GO-Schiff base material was identified using FT-IR research. Figure 4 displays the patterns of all functional groups observed at specific wavenumbers: 3440.53, 2925.99, 1639.97, 1497.86, 1427.75, 1050.95, 713.38, and 662.22 cm^{-1} . The broad peak at 3440.53 cm^{-1} corresponds to the stretching vibration of the -OH, while the peak at 2925.99 cm^{-1} is associated with the -CH₂ group. The peak detected at 1639.97 cm^{-1} corresponds to the C=N pattern, which arises from the interactions between aldehyde and silanized GO. The peak around 1497.86 cm^{-1} is often associated with the presence of a benzene ring. The peaks observed at 1427.75 and 1050.95 cm^{-1} corresponded to the Si-O-C group and the conjugated Si-O-Si group, respectively. The presence of iodine on the C-Cl ring was detected at a wavenumber of 713.38 cm^{-1} .

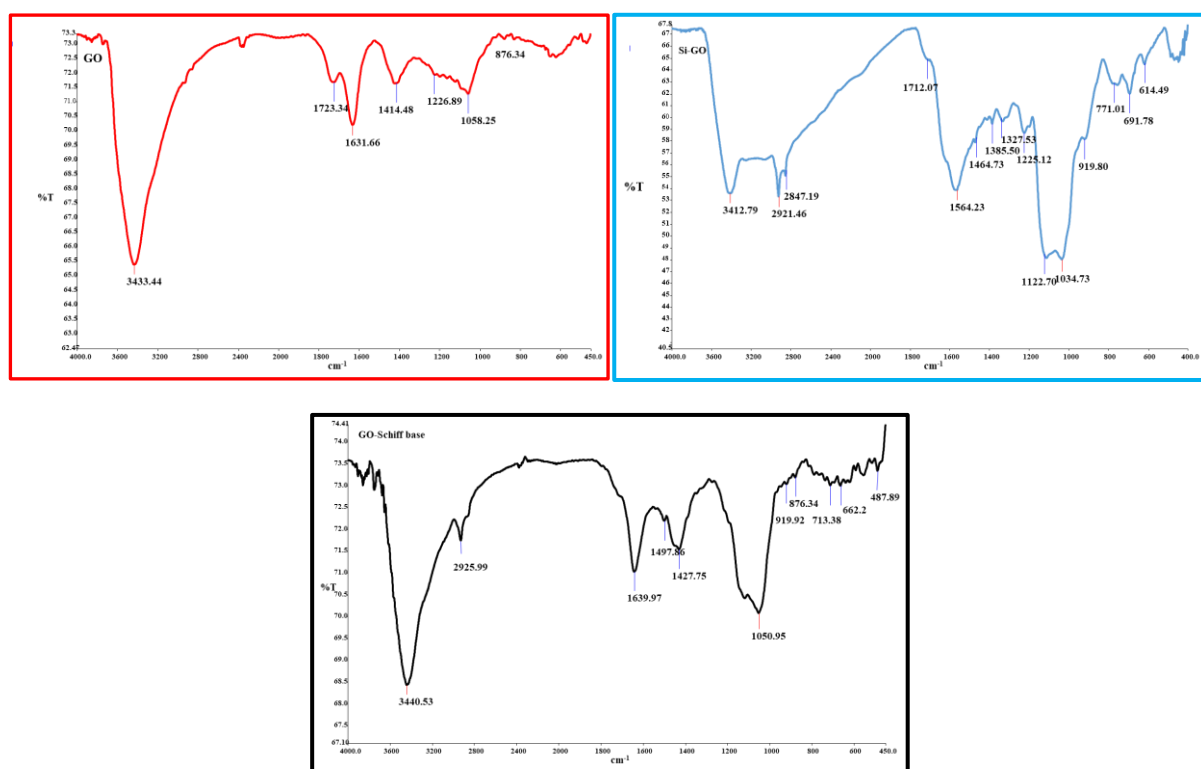


Figure 4. FT-IR Spectrums of GO, Si-GO and GO-Schiff Base

The crystal structures of the materials examined in this study were identified using the Philips X'Pert Pro X-ray diffractometer (XRD) equipped with Cu-K α radiation. The X-ray diffraction patterns of the synthesized graphene oxide, silanized GO, and hybrid material are seen. The XRD pattern of the graphene oxide may be found in the Supplementary File (Fig. S2). There is a clear and prominent peak observed at an angle of $2\theta = 10.21$, which corresponds to an interlayer spacing of 8.65 Å. The successful achievement of exfoliation is demonstrated. In addition, a clear and separate peak is observed in the Supplementary File (Fig. S3), which is characterized by its broad shape. In addition, a weak diffraction peak of the Silanized-GO material is observed at $2\theta = 22.5$ (3.94Å) and $2\theta = 43.6$ (2.07 Å), indicating the distance between the Si-GO layers in the plane. These pictures illustrate the

successful adhesion of silane groups to the surface of GO. The XRD spectrum of the G-hybrid material is presented in the Supplementary File (Fig. S4). Within this spectrum, the distinct peak of GO is no longer discernible, and instead, two additional diffraction peaks can be identified at $2\theta = 43.80$ and $2\theta = 51.40$, which correspond to interplanar distances of 2.06 and 1.77 Å, respectively. These peaks are most likely caused by the hybrid material.

The structure analysis of GO and imine-G hybrid was performed utilizing high-resolution images acquired from transmission electron microscopy mode (HRTEM) with a Joel JEM2100F TEM. The transmission electron microscope (TEM) achieves a point resolution of 0.18 nm when operated at 200 kV and at room temperature. The data are contained within the Supplementary File (Fig. S5). The dimensions of the GO sheet, which are roughly 2 μm in diameter, are detected on a holey carbon film. The core area of the sheet has a pristine and even surface, whilst the borders demonstrate creasing and curling, exposing consistent circular patterns and the sheet's several layers. The detection of the GO is consistent with the observations reported for films composed of many layers of graphene. The HRTEM image in the Supplementary File (Fig. S5b) shows lattice fringes present at the edges of GO. The measured distance between adjacent fringes was around 5 nm, which surpasses the predicted interplanar distance of graphite, calculated to be 0.34 nm. The distance is determined by the existence of functional groups, such as oxygen. The GO-hybrid material was produced by combining Silanized-GO with 3,5-dichloro-salicylaldehyde in a solution of ethanol. The resultant product was analyzed at a wavelength of 200 nm. Upon analyzing the structure of the materials, it is clear that around 50% of the surface is a result of the interaction between 3-(trimethoxysilyl) propylamin and aldehyde. This interaction leads to the creation of a C=N bond, which signifies the production of a hybrid substance.

The morphology of GO was analyzed using SEM, as depicted in Figure 5(a). The oxygen-containing groups were observed on the surface of the GO nanocomposite. Furthermore, the presence of agglomerations serves as evidence for the high surface area of GO, as it indicates the existence of layers. The oxygen-containing groups are analyzed in further detail using energy dispersive X-rays, which provide information about the elemental composition of a compound, as depicted in Figure 5(b). The Supplementary File's Table S1 shows that 63.48 percent of GO was derived from carbon atoms, whereas about 22.88 percent was derived from oxygen. In Figure 2(b), there were traces of contaminants such as chlorine and sulfur. The lack of oxygen indicates that the oxidation process was successfully carried out using H₂SO₄ and HCl baths for the required duration.

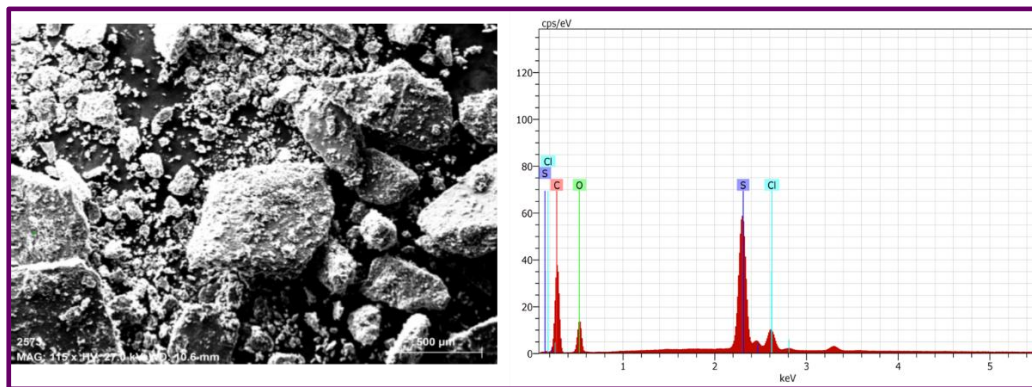


Figure 5. a. SEM and b. EDX Analysis of Graphene Oxide Nanosheets

The silanized graphene oxide was examined using a SEM. Following the silanization process, the surface of GO exhibits similar changes, including a wrinkled form and the presence of layered silane groups that are expected to anchor onto the surface. This is seen in Figure 6(a), which shows agglomerates of silanized GO. The remaining compounds were identified using EDX, which revealed a decrease in the presence of oxygen-included groups after undergoing a silanization process. The carbon and oxygen percentages were provided as 42.38 and 15.93, respectively, in the Supplementary File Table S2. Nevertheless, we successfully managed a sudden and significant increase, depicted as silane in Figure 6. Furthermore, it was demonstrated that the successful bonding between 3-(trimethoxysilyl)propylamine and GO took place. The elution of methanol during the silanization processes resulted in a reduction of the remaining contaminants.

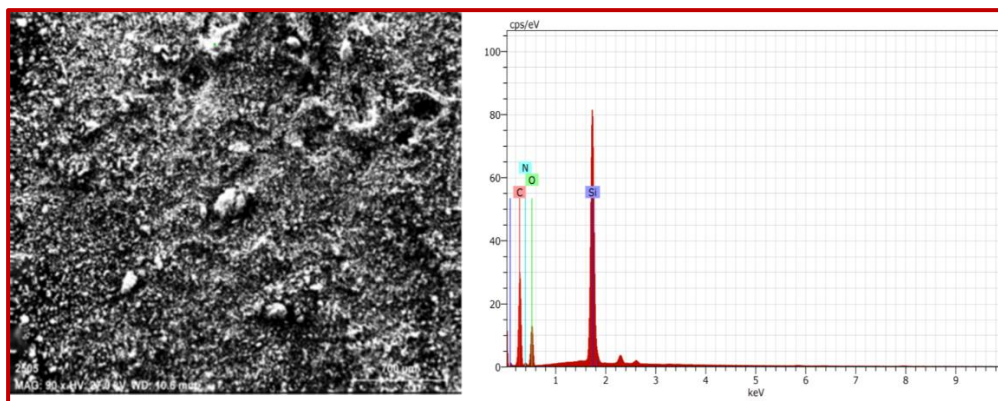


Figure 6. Observations of Silanized-Graphene Oxide Using SEM EDX

The surface morphology of the produced GO-Schiff base material was examined using SEM, and the average surface roughness was measured to be 70 micrometers, as shown in Figure 7 (a). The effective interaction between silanized GO and 3,5-dichloro-salicylaldehy can be confirmed by the presence of agglomerid and cylindric forms. The functional content of the ultimate molecule was analyzed using EDX spectroscopy. The presence of aldehydes on the surface of the graphene was confirmed by the observation of strong, sharp peaks of silane and chlorine. The carbon and oxygen content of the aldehydes increased, with percentages of 47.80% and 23.09% respectively, as shown in the Supplementary File Table S3. Additionally, Figure 7(b) clearly demonstrates a decrease in impurities after each dilution step.

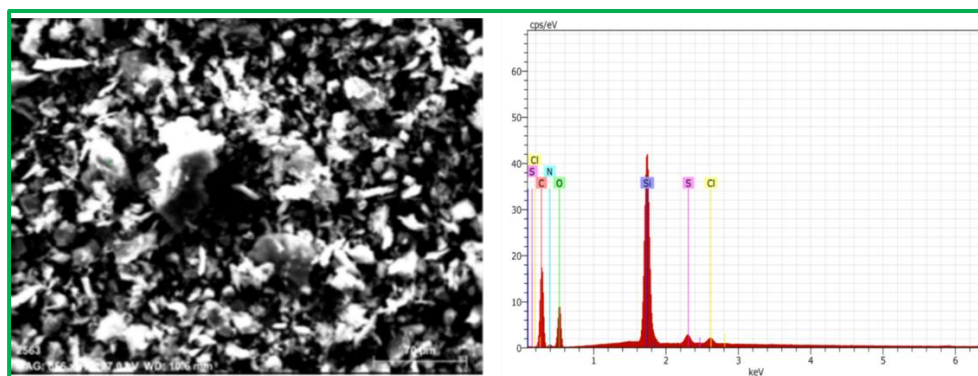


Figure 7. The Graphene Oxide-Schiff Base Material was Analyzed Using SEM and EDX

The TGA, DTA, and DTG curves of graphite G were conducted under an inert atmosphere using nitrogen within the temperature range of 20 to 900 degrees Celsius, as depicted in Figure 8. The thermal curves of the graphite indicate that water molecules adsorbed in its structure are released within the temperature range of 50–100 °C. Furthermore, during a temperature range of 100–200 °C, the water molecules responsible for crystallization are evaporated. Following this interval, the graphite continues to experience a decrease in mass until it reaches a temperature of 850 °C.

The thermal characteristics of GO have been analyzed using TGA. The object had been exposed to a controlled environment without any reactive substances present, within a temperature range of 20–900 °C. The TGA, DTA, and DTG curves are depicted in Figure 8. Upon examining the TG curve, it becomes evident that the mass of GO begins to diminish at very low temperatures, specifically around 40–50 °C. Subsequently, at a temperature of 200 °C, the process of breaking down GO commenced by eliminating acidic functional groups and residues. The majority of mass was lost between the temperature range of 100-200 °C. The TGA revealed a gradual decrease in mass of the graphene samples between 300 and 600°C, indicating an enhanced thermal stability following the removal of oxygen-containing functional groups during the reduction process.

The silanization process of GO was carried out in a controlled environment using nitrogen gas within the temperature range of 20–900 °C. Figure 8 shows the TGA, DTA, and DTG curves at 120 °C. The mass of the silanized GO

reduced significantly as a consequence. The silane groups undergo gradual decomposition starting at temperatures close to 400 °C and continue to disintegrate till reaching 900 °C.

The ultimate substance was designated as GO. The thermal properties of Schiff base hybrid compounds were assessed in a controlled environment of nitrogen gas, within a temperature range of 100–900 °C. The resulting TGA, DTA, and DTG curves are presented in Figure 8. The TGA curve, which illustrates the process of breakdown, is observed at four distinct levels. In the first and second tiers, the water molecules exhibiting a crystalline structure underwent evaporation. Decomposition of the organic component begins at the 3rd and 4th levels and persists until reaching a temperature of 900 °C.

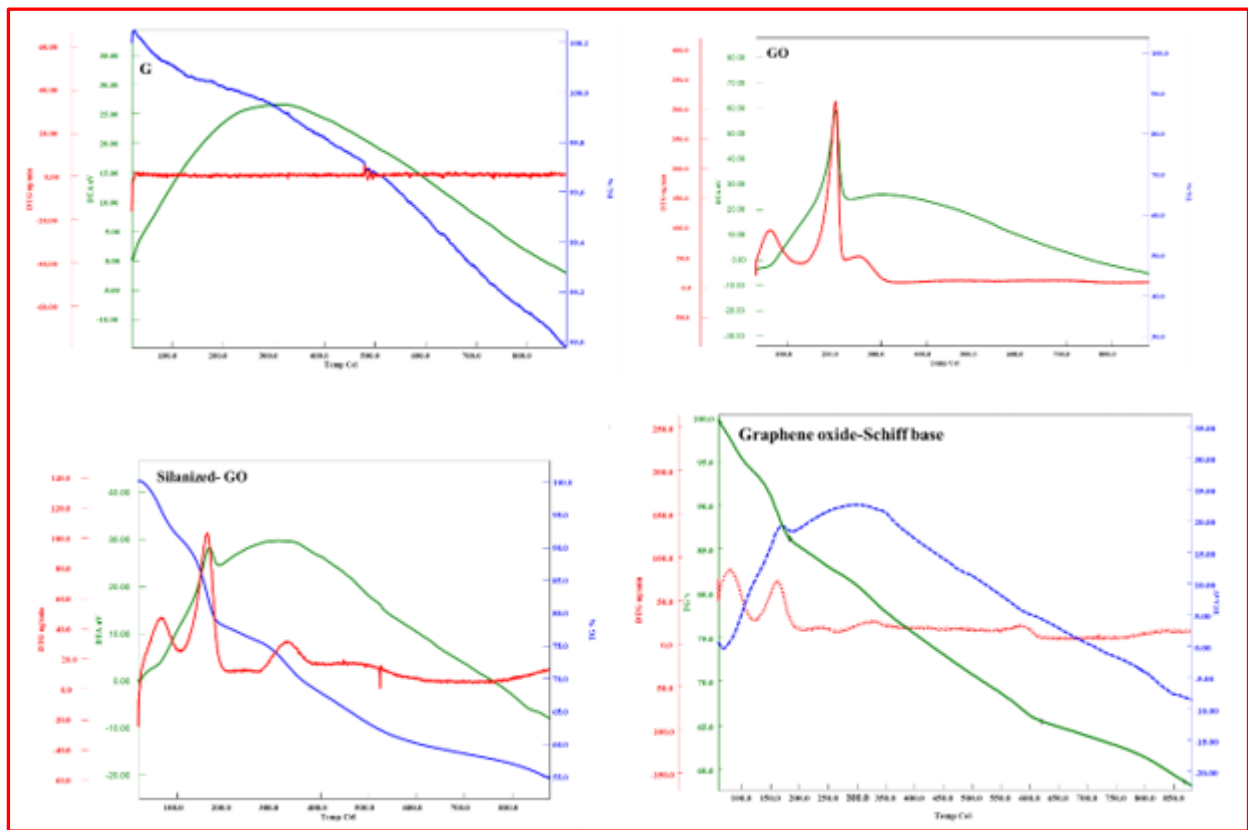


Figure 8. Thermodynamic Analysis of G, GO, GO-Schiff Base and Silanized-GO Material

Studies on The Process of Adsorption and Desorption

The adsorption of Pb(II) and Hg(II) ions was conducted utilizing a newly synthesized GO-Schiff base material in a batch setup, from an aqueous solution. Stock solutions of Pb(NO₃)₂ and HgCl₂ salts were generated at a concentration of 1000 mg/L for each ion. The HgCl₂ salts were then diluted for use in subsequent experiments. The impact of pH, heavy metal ion concentration, contact time, and temperature on the adsorption of heavy metal ions from an aqueous environment using the GO-Schiff base material was assessed. An ICP apparatus was used to measure the amounts of Pb(II) and Hg(II) ions in aqueous samples. The equation (1) below was used to determine the maximum adsorption capacity Q_{max} (mg/g), which is the amount of metal ions adsorbed per unit mass of the GO-Schiff base material.

$$Q = [(C_0 - C_e) \cdot V] / m \quad (1)$$

C₀ (mg/L) represents the concentration of the solution before the adsorption treatment, while C_e (mg/L) represents the concentration of the solution after the adsorption process. V represents the volume of the solution in liters, and m is the mass of the GO-Schiff base hybrid material.

Effect of pH

The adsorption capability is influenced by the pH level, so it is necessary to ascertain the optimal pH range for our product. An investigation was conducted to study the adsorption of Pb(II) and Hg(II) ions using a GO-Schiff base

material under varying pH conditions. The sorption experiment was carried out for both metals at a temperature of 25 °C and with 2 h of stirring. The metal solvents were at a concentration of 25 mg/L and were tested at various pH values ranging from 3 to 11. Additionally, 25 mg of GO-Schiff base material was used. Figure 9 shows that a pH value of 7 is the most optimal for achieving the highest adsorption capacity for Pb(II) and Hg(II) ions. Furthermore, it is evident from the data that the quantity of heavy metals adsorbed rises steadily and reaches its peak at a pH level of 7. Nevertheless, the precipitation of metal ions experiences a minor reduction as the pH level exceeds 9. The metal ions undergo ion exchange interactions with H⁺ cations present in the medium at low pH, resulting in their adsorption on the surfaces of GO hybrid materials. This is the reason why the adsorption capacity is enhanced at low pH. The highest level of adsorption that can occur at a pH of 7 for Pb(II) is 24.69 mg/g, whereas for Hg(II) it is 24.483 mg/g.

Effect of Contact Time

The duration of time plays a crucial role in the adsorption process of Pb(II) and Hg(II) metal ions. It is essential to establish the optimal time period for this process. The contact time tests involved the use of GO-Schiff base material to test its effectiveness in removing Pb(II) and Hg(II) metal ions. The experiments were conducted at various application durations, ranging from 5 min to 120 min. The experiments were performed under optimal conditions, with a pH of 7 and a temperature of 25 °C. The concentration of Pb(II) and Hg(II) solutions used was 25 mg/L. Figure 9 demonstrates that the adsorption of Pb(II) and Hg(II) ions progressively rises with time, reaching a notably high level within the initial 10 min. Due to the vacancies in the adsorption sites, Pb(II) and Hg(II) can readily bind to these sites. The equilibrium period for the adsorption of Pb(II) and Hg(II) was achieved after 50 min. The optimal duration for achieving maximum adsorption capacity is 50 min for Pb(II), resulting in a capacity of 24.968 mg/g. For Hg(II), the optimal duration is again 50 min, with a capacity of 23,703 mg/g.

Effect of Temperature

The impact of temperature on the adsorption of metal ions was examined within the temperature range of 5-110 °C, at a pH of 7, for Pb(II) and Hg(II) during a duration of 50 min. Each of these metal ions was produced as a 25 mL solution containing 25 mg/L of Pb(II) and Hg(II). The data indicate that the adsorption quantities are greater at lower temperatures. The reaction between the adsorbent and metal ions is exothermic. Figure 9 demonstrates that there is a decrease in sorption for Pb(II) when the temperature rises over 50 °C. The maximum adsorption for Pb(II) is 24.703 mg/g. The sorption of Hg(II) ions exhibits an increase up to a temperature of 50°C. However, above this temperature, the adsorption capacity remains constant, and the highest amount of adsorption for Hg(II) at 50 °C is 24.25 mg/g.

Effects of Different Concentrations

During this stage, our objective is to determine the highest adsorption capacity of the GO-Schiff base material, which possesses oxygen-containing groups on its surface and functional aldehyde groups. The unique shape, characterized by its porous structure and functional groups, renders this nanocomposite highly effective as an adsorbent for Pb(II) and Hg(II). An investigation was conducted to study the adsorption of Pb(II) and Hg(II) on a hybrid material consisting of GO. The experiment involved employing 25 mL of heavy metal ion solutions with concentrations ranging from 50 to 600 mg/L. The adsorption process was carried out at optimal conditions of temperature, time, and pH, which were set at 25 °C, 60 min, and pH = 7, respectively. The samples were stirred during the adsorption process. Nevertheless, the quantity of nanocomposite is 25 milligrams. According to Figure 9, the highest amount of Pb(II) that may be adsorbed is 455.44 mg/g, while for Hg(II) it is 364.50 mg/g.

RESULT AND DISCUSSION

Heavy metals are vital for the survival of all living species, however, their long-term accumulation through consumption of food, inhalation of air, and ingestion of water can lead to the development of many ailments. While they occur naturally in the ground, they still contribute to environmental pollution. Hence, safeguarding human health necessitates the prevention of the deterioration and annihilation of these metals. Recently, several ways have been devised to minimize their ecological footprint by employing diverse techniques centered upon GO.

Adsorption is a very effective and efficient method for cleaning the environment, and graphene possesses exceptional adsorption capabilities owing to its inherent shape. Graphene is a highly promising material for effectively eliminating heavy metal ions from the air, water, and soil.

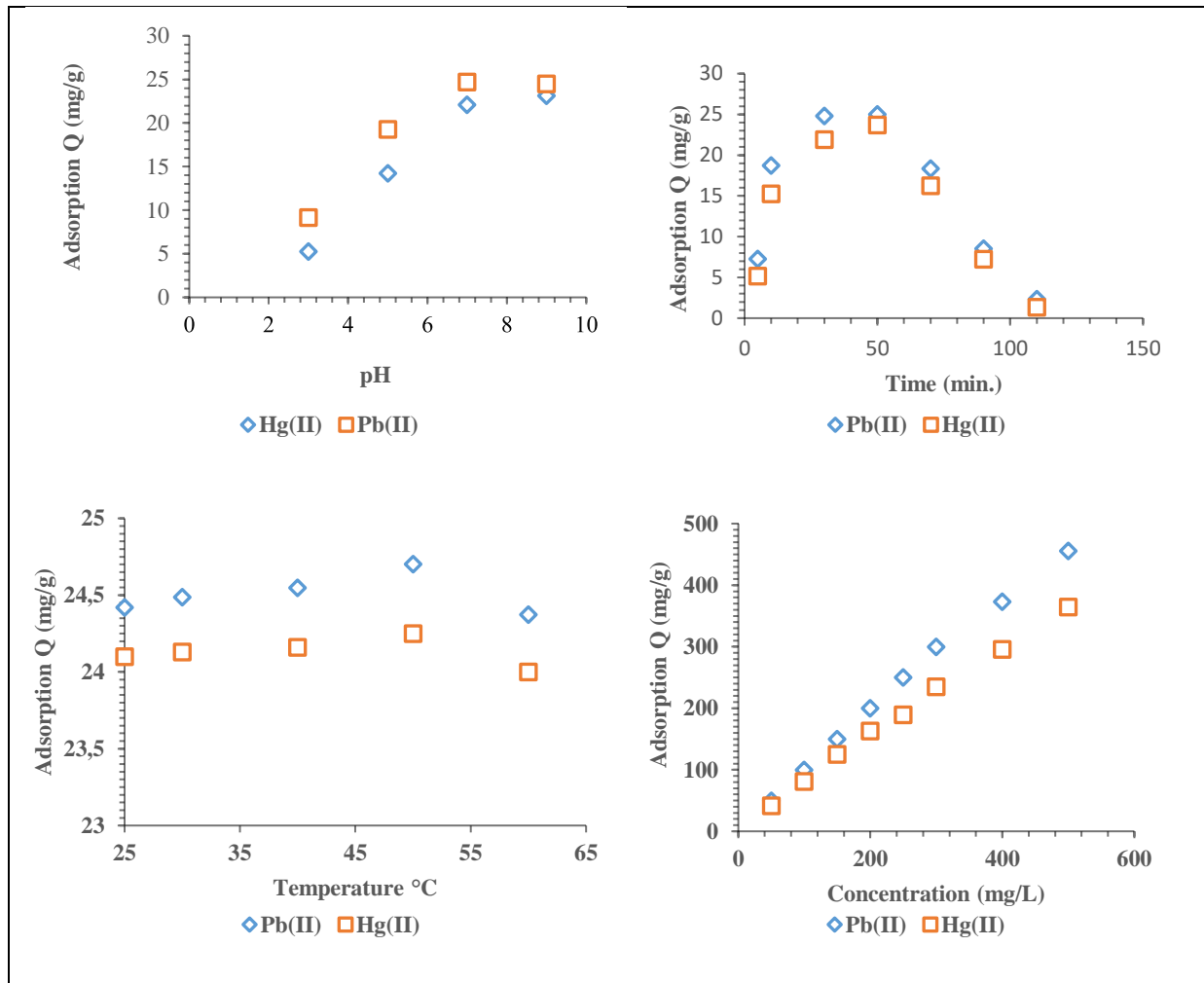


Figure 9. Effect of pH, Contact Time, Temperature, Equilibrium Concentration, on Pb(II) and Hg(II) Adsorption

This study involved the synthesis of a hybrid material based on graphene, and the investigation of its ability to remove Pb(II) and Hg(II) ions from prepared solutions. The investigations demonstrated the exceptional adsorption of Pb(II) and Hg(II) ions by graphene. The optimal working parameters were identified as a pH of 7, a temperature of 50 °C, and a duration of 50 min. The efficacy of graphene-based adsorbent material in removing heavy metal ions from aquatic environments is notable due to its cost-effectiveness, accessibility, and ability to be reused.

The findings suggest that GO and its derivatives have the potential to be used and reused as materials. The development of recyclable materials is a significant concern in various sectors of the contemporary and interconnected world, encompassing industries ranging from mobile phones to textiles. Graphene-based materials are regarded as highly promising contenders in this domain.

REFERENCES

- Abd Elnabi, M. K., Elkaliny, N. E., Elyazied, M. M., Azab, S. H., Elkhalifa, S. A., Elmasry, S., ... & Mahmoud, Y. A. G. (2023). Toxicity of heavy metals and recent advances in their removal: A review. *Toxics*, 11(7), 580. <https://doi.org/10.3390/toxics11070580>
- Ali, H., Khan, E., & Ilahi, I. (2019). Environmental chemistry and ecotoxicology of hazardous heavy metals: Environmental persistence, toxicity and bioaccumulation. *Journal of Chemistry*, 2019. <https://doi.org/10.1155/2019/6730305>
- Aliasgharpour, M., & Marjan, R. F. (2013). Trace elements in human nutrition: A review. *The Journal of Medical Investigation*. 2(3), 115-128. https://doi.org/10.4103/ijpvm.IJPVM_48_19

- Bal, M., Tümer, M., & Köse, M. (2024). Synthesis of reduced graphene oxide-based hybrid materials containing imine bonds: Color properties and chemosensory properties against some anions. *Materials Science and Engineering: B*, 303, 117278. <https://doi.org/10.1016/j.mseb.2024.117278>
- Balali-Mood, M., Naseri, K., Tahergorabi, Z., Khazdair, M. R., & Sadeghi M. (2021) Toxic mechanisms of five heavy metals: Mercury, lead, chromium, cadmium and arsenic. *Frontiers in Pharmacology*, 12, 643972. <https://doi.org/10.1016/j.mseb.2024.117278>
- Bhattacharya, P. T., Misra, S. R., & Hussain, M. (2016). Nutritional aspects of essential trace elements in oral health and disease: *An extensive review. Scientifica*, 2016. <https://doi.org/10.1155/2016/5464373>
- Gabriel, M., & Elena, L. U. (2022). "Toxicity of Heavy Metals," Chapters, in: Hosam M. Saleh & Amal I. Hassan (ed.), *Environmental Impact and Remediation of Heavy Metals*, IntechOpen. <https://doi.org/10.5772/intechopen.102441>
- Hou, S., Su, S., Kasner, M. L., Shah, P., & Patel K., (2010). Formation of highly stable dispersions of silane-functionalized reduced graphene oxide *Chemical Physics*, 501(1-3), 68-74. <https://doi.org/10.1016/j.cplett.2010.10.051>
- Hummers, Jr., William, S., & Richard E. O. (1958). Preparation of graphitic oxide. *Journal of the American Chemical Society*, 80(6), 1339-1339. <https://doi.org/10.1021/ja01539a017>
- Ingrassia, E. B., Fiorentini, E. F., Wuilloud, R. G., Agostini, E., Oller, A. L. W., & Escudero, L. B. (2024). Bionanomaterial composed of Bradyrhizobium japonicum and graphene oxide for determination of mercury in water and fruit juice samples. *Journal of Food Composition and Analysis*, 127, 105967. <https://doi.org/10.1016/j.jfca.2024.105967>
- Jamali, M. R., Assadi, Y., Shemirani, F., & Hosseini, M. R. M. (2006). Synthesis of salicylaldehyde-modified mesoporous silica and its application as a new sorbent for separation, preconcentration and determination of uranium by inductively coupled plasma atomic emission spectrometry. *Analytica chimica*, 579(1), 68-73. <https://doi.org/10.1016/j.aca.2006.07.006>
- Lucena, R. (2023). Janusz Pawliszyn (Ed.): Evolution of solid phase microextraction technology. <https://doi.org/10.1007/s00216-023-04959-2>
- Masindi, V., & Muedi, K.L. (2018) Environmental contamination by heavy metals. In: Saleh HEDM, Aglan RF, editors. *Heavy Metals*. Chichester: IntechOpen. 115-133. <https://dx.doi.org/10.5772/intechopen.76082>
- Mitra, S., Chakraborty, A.J., Tareq, A.M., Emran, T.B., Nainu, F., Khusro, A., Idris, A.M., Khandaker, M.U., Osman, H., Alhumaydhi, F.A., & Jesus S.G. (2022). Impact of Heavy Metals on the Environment and Human Health: Novel Therapeutic Insights to Counter the Toxicity. *J. King Saud Univ.-Sci.* 34(3), 101865. <https://doi.org/10.1016/j.jksus.2022.101865>
- Pasupuleti, R. R., & Huang, Y. L. (2023). Recent applications of atomic spectroscopy coupled with magnetic solid-phase extraction techniques for heavy metal determination in environmental samples: A review. *Journal of the Chinese Chemical Society*, 70, 1326–1337. <https://doi.org/10.1002/jccs.202300029>
- Zhou, W., Wiczorek, M. N., Javanmardi, H., & Pawliszyn, J. (2023). Direct solid-phase microextraction-mass spectrometry facilitates rapid analysis and green analytical chemistry. *TrAC Trends in Analytical Chemistry*, 166, 117167. <https://doi.org/10.1016/j.trac.2023.117167>